

An Asymptotically Derived Boundary Element Method for the Helmholtz Equation

Eldar Giladi

Department of Mathematical Sciences
RPI, Troy NY 12180
gilade@rpi.edu

Joseph B. Keller

Departments of Mathematics and
Mechanical Engineering
Stanford University, Stanford CA 94305

Abstract

We present an asymptotically derived boundary element method for the Helmholtz equation in exterior domains, in which the basis functions are asymptotically derived. Each basis function is the product of a smooth amplitude and an oscillatory phase factor, like the asymptotic solution. The phase factor is determined a-priori by using arguments from geometrical optics and the geometrical theory of diffraction, while the smooth amplitude is represented by high order splines. Our approach accounts for all the components of the scattered field namely the reflected, shadow forming and diffracted fields, and we demonstrate that it is substantially more accurate than an approach which accounts for the reflected field only. Two types of diffracted basis functions are presented: the first accounts for the dominant oscillatory behavior in the shadow region while the second also accounts for the decay of the amplitude there. Although the method is applicable to a variety of scatterers, we focus our attention here on scattering from smooth convex bodies in two dimensions. Our computations with a conducting circular cylinder demonstrate that the number of unknowns necessary to achieve a given accuracy with this new basis is virtually independent of the wave-number.

1 Introduction

The numerical solution of scattering problems modeled by the Helmholtz equation in exterior domains, is exceedingly difficult if not computationally intractable by standard computational schemes, for frequencies in the mid and high regime. Indeed, for three dimensional problems the number of unknowns in both the finite difference and the finite element methods scales like the cube of ka , where k is the wave number and a is a typical dimension of the scatterer, while in a boundary integral method it scales like the square of ka . In recent years various researchers [1–10] have developed special variants of the finite element and the boundary integral equation methods which reduce the computational complexity of the problem. The common feature among these algorithms is the use of a-priori knowledge regarding the oscillatory nature of the solution in the design of the numerical scheme.

In this paper we develop a boundary element collocation method for the integral formulation of the Helmholtz equation, in which the basis functions are asymptotically derived. Each basis function is the product of a smooth amplitude and a highly oscillatory phase factor, like the asymptotic solution. The phase factor is determined a-priori by geometrical optics (GO) and the the geometrical theory of diffraction (GTD) [11], while the smooth amplitude is a high order spline. Each basis function is associated with a field: reflected, shadow forming, diffracted, multiply diffracted etc... and we use GO and GTD to determine which fields are present. The method is applicable to a variety of scattering problems, but in this paper we focus on smooth convex scatterers in two dimensions, and we demonstrate the method on a conducting circular cylinder.

Our method is analogous to the finite element method which we developed for the Helmholtz equation in [8], in which GO and GTD where used to determine the components of the scattered field, and the oscillatory phase factor of the associated basis functions. It extends the approach taken in [1, 4, 10] for the integral equation, in that our basis functions account for all the fields present, including the diffracted fields. This greatly improves the accuracy of the computed results, and enables the method

Report Documentation Page

*Form Approved
OMB No. 0704-0188*

Public reporting burden for the collection of information is estimated to average 1 hour per response, including the time for reviewing instructions, searching existing data sources, gathering and maintaining the data needed, and completing and reviewing the collection of information. Send comments regarding this burden estimate or any other aspect of this collection of information, including suggestions for reducing this burden, to Washington Headquarters Services, Directorate for Information Operations and Reports, 1215 Jefferson Davis Highway, Suite 1204, Arlington VA 22202-4302. Respondents should be aware that notwithstanding any other provision of law, no person shall be subject to a penalty for failing to comply with a collection of information if it does not display a currently valid OMB control number.

1. REPORT DATE 24 FEB 2004	2. REPORT TYPE N/A	3. DATES COVERED -	
4. TITLE AND SUBTITLE An asymptotically derived boundary element method for the Helmholtz equation		5a. CONTRACT NUMBER	
		5b. GRANT NUMBER	
		5c. PROGRAM ELEMENT NUMBER	
6. AUTHOR(S)		5d. PROJECT NUMBER	
		5e. TASK NUMBER	
		5f. WORK UNIT NUMBER	
7. PERFORMING ORGANIZATION NAME(S) AND ADDRESS(ES) Department of Mathematical Sciences RPI, Troy ,NY 12180		8. PERFORMING ORGANIZATION REPORT NUMBER	
9. SPONSORING/MONITORING AGENCY NAME(S) AND ADDRESS(ES)		10. SPONSOR/MONITOR'S ACRONYM(S)	
		11. SPONSOR/MONITOR'S REPORT NUMBER(S)	
12. DISTRIBUTION/AVAILABILITY STATEMENT Approved for public release, distribution unlimited			
13. SUPPLEMENTARY NOTES See also ADM001763, Annual Review of Progress in Applied Computational Electromagnetics (20th) Held in Syracuse, NY on 19-23 April 2004., The original document contains color images.			
14. ABSTRACT			
15. SUBJECT TERMS			
16. SECURITY CLASSIFICATION OF:			17. LIMITATION OF ABSTRACT
a. REPORT unclassified	b. ABSTRACT unclassified	c. THIS PAGE unclassified	UU
			18. NUMBER OF PAGES 8
			19a. NAME OF RESPONSIBLE PERSON

to be extended to problems where the previous approaches are not effective. Our method is also similar to those presented in [2, 3, 9] for discretizing the boundary integral equation, with basis functions which are the product of polynomials and plane waves. The latter approach [9] draws its roots in the partition of unity finite element method [5, 12] for the partial differential equation, and it makes use of a multiple number of plane waves on each element, in directions which uniformly cover the unit circle. In our approach, both the number of basis functions and their associated phase factors are determined by GO and GTD. Hence, the phase factors are not necessarily plane waves, and each basis function is very effective at representing at least one component of the scattered wave.

2 Problem formulation and discretization

2.1 Problem formulation

We consider scattering by a convex curve Γ , of a time harmonic plane wave of unit amplitude, $\exp(i\mathbf{k} \cdot \mathbf{x})$, where \mathbf{k} is a vector of magnitude k , and $\mathbf{x} = (x, y)$. Hence we seek a solution to

$$\Delta u + k^2 u = 0, \quad (1)$$

in the unbounded domain exterior to Γ . We seek u of the form

$$u = e^{i\mathbf{k} \cdot \mathbf{x}} + u^s, \quad (2)$$

where $\exp(i\mathbf{k} \cdot \mathbf{x})$ and u^s are the incident and scattered fields, respectively. Here we impose on u a Dirichlet condition and on u^s the Sommerfeld radiation condition

$$u(x, y) = 0, \quad (x, y) \in \Gamma, \quad (3)$$

and

$$\lim_{r \rightarrow \infty} r^{1/2} \left(\frac{\partial u^s}{\partial r} - iku^s \right) = 0. \quad (4)$$

The computational problem which we wish to solve is (1) for u^s , subject to the conditions

$$u^s = -\exp(i\mathbf{k} \cdot \mathbf{x}), \quad (x, y) \in \Gamma, \quad (5)$$

and (4). We derive an integral equation for this problem in a standard fashion (see: [13]),

$$\int_{\Gamma} \frac{\partial u^s(\mathbf{x})}{\partial n} G(\mathbf{x}, \xi) d\mathbf{x} = - \int_{\Gamma} \exp(i\mathbf{k} \cdot \mathbf{x}) \frac{\partial G(\mathbf{x}, \xi)}{\partial n} d\mathbf{x} + \frac{\exp(i\mathbf{k} \cdot \xi)}{2}, \quad (6)$$

where the free space Green's function $G(\mathbf{x}, \xi) = (i/4)H_0^1(k\|x - x_i\|)$, and H_0^1 is the Hankel function of the first kind. For the purpose of demonstrating the accuracy of this approach, it was not necessary to consider more stable formulations such as the combined fields approach [14]. Indeed, for the wave numbers considered here the accuracy is excellent as we shall see.

2.2 Discretization by a boundary element method

We shall approximate $\partial u^s / \partial n$ with a boundary element method. Hence, we introduce basis functions $N_j(\mathbf{x})$, $j = 0, \dots, N-1$ defined on Γ and look for an approximation of the form

$$\frac{\partial u^s(\mathbf{x})}{\partial n} \approx \sum_{j=0}^{N-1} c_j N_j(\mathbf{x}). \quad (7)$$

In order to obtain a system of equations for the coefficients c_j in (7) we substitute the right side of (7) for $\partial u^s / \partial n$ into (6), and evaluate the terms in this equation at N distinct collocation points ξ_0, \dots, ξ_{N-1} . This yields the system of equations

$$A\vec{c} = \vec{g},$$

$$A_{i,j} = \int_{\Gamma_j} N_j(\mathbf{x}) G(\mathbf{x}, \xi_i) d\mathbf{x}, \quad g_i = - \int_{\Gamma} \exp(i\mathbf{k} \cdot \mathbf{x}) \frac{\partial G(\mathbf{x}, \xi_i)}{\partial n} d\mathbf{x} + \frac{\exp(i\mathbf{k} \cdot \xi_i)}{2}. \quad (8)$$

where Γ_j is the support of N_j on Γ .

We assume here that the scatterer Γ is parametrized by the mapping

$$\Gamma(s), \quad a \leq s \leq b, \quad \Gamma(a) = \Gamma(b). \quad (9)$$

Then, we define the *standard basis functions* and collocation points by first introducing the mesh points s_i $i = 0, \dots, N-1$, in $[a, b]$ and the associated B-splines $M_i^l(s)$ of polynomial degree l , centered at s_i . The standard basis functions N_i^l , and collocation points ξ_i are defined on Γ by

$$\xi_i = \Gamma(s_i), \quad (10)$$

$$N_i^l(\mathbf{x}) = M_i^l(\Gamma^{-1}(\mathbf{x})), \quad \text{where } \mathbf{x} \in \Gamma. \quad (11)$$

2.3 Asymptotically derived basis functions

The asymptotic theory for problem (1)-(4), based on GO and the GTD, is described in detail in [15,16]. Here, we review the essential elements of that theory necessary for the development of asymptotic basis functions. Additional relevant details can be found in [8,17]. In the asymptotic theory, one seeks the solution u^s in (2) as a superposition of the form

$$u^s(x, y) = \sum_{l=1}^L A_l(x, y) \exp(ikS_l(x, y)). \quad (12)$$

Here L is the number of fields, and for a smooth convex scatterer there are four terms

$$u^s = u^r + u^{sf} + u^{d+} + u^{d-}. \quad (13)$$

They are the reflected field u^r , the shadow forming field u^{sf} , and two diffracted fields u^{d+} , u^{d-} which are associated with special points of Γ . Specifically, each incident ray which is tangent to the cylinder gives rise to a surface diffracted ray which travels around Γ starting at the point of diffraction. When the scatterer is a circular cylinder of radius 1 centered at $(0, 0)$ and $\mathbf{k} = (1, 0)$ in (2), the points of tangency are $(0, 1)$ and $(0, -1)$, respectively. Moreover, u^{sf} satisfies $u^{sf} + u^i = 0$ in the region $x \geq 0$, $|y| \leq 1$, so $u^{sf} = -\exp(ikx)$ there. In our formulations it contributes an additional term

$$-k/4 \int_{\Gamma \setminus \Gamma_r} \cos \theta \exp(ik\mathbf{x}) H_0(k\|\mathbf{x} - \mathbf{x}_i\|) d\mathbf{x}, \quad \theta = \arg(\mathbf{x}),$$

to g_i in (8).

Each field in (13) has the form

$$A(x, y) \exp(ikS(x, y)), \quad (14)$$

where the amplitude A is smooth and the phase $S(x, y)$ can be determined by the ray method. Only the reflected and shadow forming fields are non-zero on the surface of the scatterer but the normal derivative of all fields is non-zero there. With Γ the unit circle

$$\Gamma(s) = (\cos s, \sin s), \quad (15)$$

and $\mathbf{k} = (1, 0)$ in (2) we have

$$S^r(x, y) = x, \quad S^{sf}(x, y) = x, \quad S^{d^+} = s^+(x, y), \quad S^{d^-} = s^-(x, y), \quad s^+, s^- \geq 0. \quad (16)$$

The functions s^+ and s^- are respectively the distances traveled around the cylinder by the surface diffracted rays from the diffraction points $(0, 1)$ and $(0, -1)$ in the clockwise and counterclockwise directions to the point (x, y) . The functions s^+, s^- are multivalued and unbounded because surface diffracted rays travel an infinite number of times around the cylinder. This is easily overcome as explained in [8, 17], and s^+, s^- in (16) are the shortest distances. Moreover, the quantities $\partial u^{d^+}/\partial n$ and $\partial u^{d^-}/\partial n$ decay exponentially by a damping factor $D(s^+)$ and $D(s^-)$, respectively (see: [16, 17]) where

$$D(s) = \exp(i\tau_0 k^{1/3} s), \quad \text{and} \quad \tau_0 = \exp(i\pi/3.0) (9\pi/2)^{2/3} / 4.0. \quad (17)$$

It follows that $\partial u^{d^+}/\partial n$ is exponentially smaller than $\partial u^{d^-}/\partial n$ when $s^+ > \pi/2$ and $k \rightarrow \infty$, and vice versa when $s^- > \pi/2$. However, both $\partial u^{d^+}/\partial n$ and $\partial u^{d^-}/\partial n$ will be non-negligible compared to each other in the neighborhood of $(x, y) = (1, 0)$ where $s^+ = s^- = \pi/2$.

This leads to a decomposition of Γ into four zones

$$\Gamma_r = \{\Gamma(s) \mid \pi/2 \leq s \leq 3\pi/2\}, \quad \Gamma_{d^+} = \{\Gamma(s) \mid \alpha \leq s \leq \pi/2\}, \quad (18)$$

$$\Gamma_{d^-} = \{\Gamma(s) \mid 3\pi/2 \leq s \leq 2\pi - \alpha\}, \quad \Gamma_o = \{\Gamma(s) \mid -\alpha \leq s \leq \alpha\}, \quad (19)$$

with α a small positive scalar. In each zone we use basis functions of the form

$$\hat{N}_1(j, l, t, \mathbf{x}, k) = N_j^l(\mathbf{x}) \exp(ikS^t(\mathbf{x})), \quad \text{for} \quad \mathbf{x} \in \Gamma_t \quad t \in \{d^+, d^-, r\}, \quad (20)$$

where S^t is defined in (16), $N_j^l(\mathbf{x})$ in (11) and Γ_t in (18) and (19). In the overlap region Γ_o we use basis functions associated with both Γ_{d^+} and Γ_{d^-} . We also introduce the modified basis functions in $\Gamma_{d^+}, \Gamma_{d^-}, \Gamma_o$, which include the decay (17)

$$\hat{N}_2(j, l, t, \mathbf{x}, k) = N_j^l(\mathbf{x}) \exp(ikS^t(\mathbf{x}))D(S^t(\mathbf{x})), \quad \text{for} \quad \mathbf{x} \in \Gamma_t \quad t \in \{d^+, d^-\}. \quad (21)$$

In our calculations we shall compare the performance of the basis functions (20) and (21) with

$$\hat{N}_3(j, l, \mathbf{x}, k) = N_j^l(\mathbf{x}) \exp(ik\mathbf{x}), \quad \mathbf{x} \in \Gamma, \quad (22)$$

which are based on the GO ansatz used in [1, 4, 10].

2.4 Implementation details

Several issues need to be considered in a numerical implementation in order for the method to be efficient and accurate, and they are presented in detail in [17]. The numerical integration of the oscillatory integrals in (8) are computed by specialized quadrature rules, in time virtually independent of k . Preconditioning of the system (8) by the norm of each column, when basis functions (21) are used, is required. Improved efficiency can be achieved by mesh adaptivity, as discussed in [8], and the use of variable order splines. Appropriate measures need to be taken to avoid dependence between basis function in the overlap region for small values of k , as described in [8, 17].

3 Numerical calculations

We now compare the accuracy of the numerical approximation to $\frac{\partial(u^s - u^{sf})}{\partial n}$ obtained with each of the three families of basis functions (20), (21) and (22), in which N_j^l are B-splines of order $l = 5$. The number of discretization points is 250.

Figure 1 presents the absolute value of the real and imaginary parts of the exact and computed solutions at the nodes of the grid in the shadow region, for $k = 750$. In most of the shadow region bases (20) and (21) yield excellent results while basis (22) provides an accurate solution in only half of that region. Basis (21) is slightly better than (20). All three approximations agree to graphical accuracy in the illuminated region which we do not show here. Basis (22) is accurate near the shadow boundary because the phase of the diffracted field, s^+ , is well approximated there by x , as indicated by the relation

$$x = \cos(\pi/2 - s^+) = s^+ - \frac{s^{+3}}{6} + O(s^{+5}). \quad (23)$$

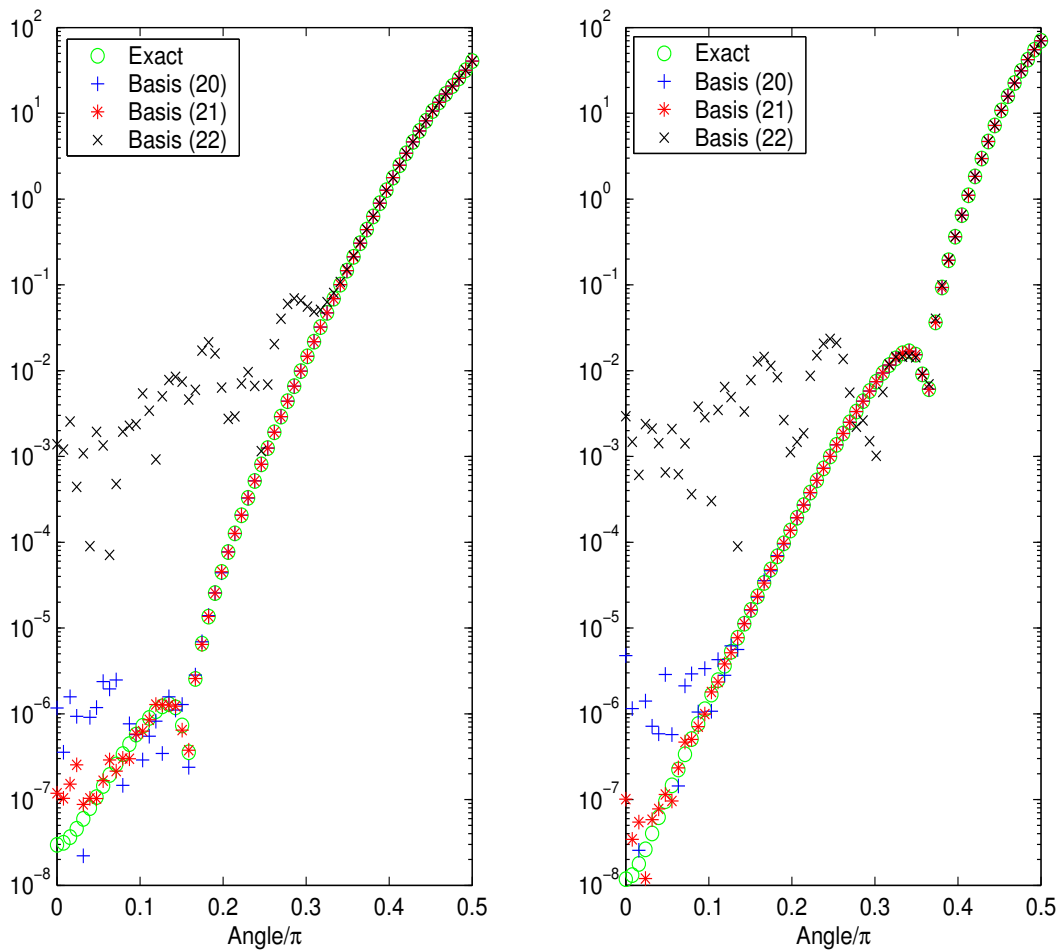


Figure 1: The absolute value of the real and imaginary parts of the exact and computed values of $\partial(u^s - u^{sf})/\partial n$ for $k = 750$, in the left and right panels respectively. The exact solution, and approximations with basis (20)-(22) are plotted with o, +, *, and ×, respectively.

Table 2 presents the error between exact and computed values of $\frac{\partial(u^s - u^{sf})}{\partial n}$, on the cylinder surface over the range $k = 10 - 5000$, evaluated at the nodes of the grid. Both the maximum and median errors are presented. The superiority of bases (20) and (21) over (22) is apparent. Basis (21) provides an order of magnitude greater accuracy than basis (21).

k	$\ \text{error}\ _\infty$			Median $ \text{error} $		
	Basis (20)	Basis (21)	Basis (22)	Basis (20)	Basis (21)	Basis (22)
10	2.66e-07	4.82e-07	1.19e-08	3.45e-09	6.88e-09	5.52e-10
50	7.67e-04	9.88e-04	8.54e-06	6.02e-05	7.71e-05	5.30e-07
100	6.53e-04	5.61e-04	3.07e-04	3.47e-05	3.44e-05	3.20e-05
250	6.99e-05	3.82e-05	3.42e-02	3.91e-06	1.60e-06	4.26e-03
500	1.68e-05	1.73e-06	5.63e-02	6.96e-07	9.57e-08	5.83e-03
1000	1.09e-04	1.49e-05	5.41e-01	3.06e-06	6.27e-07	1.01e-01
2000	7.20e-04	1.34e-04	3.99e+00	1.49e-05	4.37e-06	9.29e-01
2500	1.33e-03	2.63e-04	1.16e+01	2.33e-05	9.81e-06	2.12e+00
5000	8.99e-03	2.24e-03	2.31e+01	4.30e-04	7.13e-05	4.83e+00

Figure 2: The maximum and median *error* at the discretization points on the surface of the cylinder.

The increase in the error as a function of k which can be seen in Table 2, is due to the fact that $\left| \frac{\partial(u^s - u^{sf})}{\partial n} \right|$, is proportional to k in the illuminated region. This does not affect by much the error in the total field $u^i + u^s$ in the exterior of the cylinder as indicated in Table 3. This table presents the maximum and median *relative error* in $|u^i + u^s|$ for a set of points A in the illuminated region exterior to the cylinder defined by

$$A = \{(r_i \cos \theta_j, r_i \sin \theta_j) \mid r_i = 1 + .5i, i = 1, \dots, 4, \theta_j = j2\pi/17\} \setminus \{(x, y) \mid x \leq 0, |y| \leq 1\}. \quad (24)$$

Here again we see that bases (20) and (21) are at least 4 orders of magnitude more accurate than the basis (22). Tables 3 presents the maximum and median *relative error* in $|u^i + u^s|$ for a set of points B in the shaded region exterior to the cylinder defined by

$$B = \{(r_i \cos \theta_j, r_i \sin \theta_j) \mid r_i = 1 + .5i, i = 1, \dots, 4, \theta_j = j2\pi/17\} \cap \{(x, y) \mid x \leq 3, |y| \leq 1\}. \quad (25)$$

We excluded from B points in the deep shadow close to the cylinder surface, as we did not expect basis (22) to perform well there. However, we see that throughout the shadow region it performs quite poorly, Basis (21) on the other hand is accurate to at least two significant figures even for $k = 5000$. The reduction in the number of significant digits in the shadow region as k increases is explained in [17].

k	$\ \text{relative error}\ _{\infty}$			Median $ \text{relative error} $		
	Basis (20)	Basis (21)	Basis (22)	Basis (20)	Basis (21)	Basis (22)
10	1.96e-10	4.02e-10	1.41e-11	7.99e-12	1.63e-11	1.18e-12
50	1.80e-06	2.48e-06	1.36e-08	6.73e-08	1.11e-07	1.40e-09
100	1.14e-06	1.11e-06	2.70e-06	1.22e-07	1.23e-07	4.16e-07
250	5.26e-08	2.94e-08	4.76e-05	6.26e-09	3.25e-09	5.98e-06
500	9.33e-09	1.18e-09	8.37e-05	9.08e-10	7.52e-11	5.21e-06
1000	2.06e-08	3.96e-09	5.49e-04	2.43e-09	5.24e-10	4.99e-05
2000	9.56e-08	1.31e-08	1.44e-03	2.27e-09	4.82e-10	1.87e-04
2500	1.91e-07	2.45e-08	1.95e-03	8.69e-09	1.89e-09	3.82e-04
5000	7.17e-07	8.29e-08	2.59e-03	1.87e-08	3.29e-09	4.33e-04

Figure 3: The maximum and median *relative error* on the set A of points in the illuminated region.

k	$\ \text{relative error}\ _{\infty}$			Median $ \text{relative error} $		
	Basis (20)	Basis (21)	Basis (22)	Basis (20)	Basis (21)	Basis (22)
10	4.51e-10	9.13e-10	1.14e-11	2.13e-10	4.31e-10	4.46e-12
50	3.99e-06	4.56e-06	2.37e-08	1.40e-06	1.60e-06	9.68e-09
100	1.30e-05	1.68e-05	1.70e-05	2.24e-06	2.69e-06	3.00e-06
250	5.65e-06	3.05e-06	2.99e-03	8.03e-07	3.29e-07	3.93e-04
500	2.15e-07	3.05e-08	2.89e-02	4.99e-08	9.51e-09	2.77e-03
1000	8.21e-06	2.43e-06	4.55e-01	7.33e-07	1.77e-07	4.28e-02
2000	7.86e-04	1.37e-04	8.25e+00	4.50e-06	1.14e-06	2.57e-01
2500	4.01e-03	4.73e-04	7.98e+01	3.72e-05	9.03e-06	1.03e+00
5000	1.80e-01	1.61e-02	2.11e+02	4.44e-04	1.25e-04	3.28e+00

Figure 4: The maximum and median *relative error* on the set B of points in the shaded region.

References

- [1] R. M. James. A contribution to scattering calculation for small wavelengths—the high frequency panel method. *IEEE Transactions on Antennas and Propagation*, 38(10):1625–1630, 1990.
- [2] A. de la Bourdonnaye. A microlocal discretization method and its utilization for a scattering problem. *Comptes Rendus de l'Academie des Science. Paris. Serie I*, 318:385–388, 1994.
- [3] T. Abboud J. C. Nedelec and B. Zhou. Methode des equations integrales pour les hautes frequences. *Comptes Rendus de l'Academie des Science. Paris. Serie I*, 318:165–170, 1994.
- [4] K. R. Aberegg and A. F. Peterson. Application of the integral equation asymptotic phase method to two dimensional scattering. *IEEE Transactions on Antennas and Propagation*, 43(5):534–537, 1995.
- [5] J.M. Melenk and I.M. Babuška. The partition of unity finite element method: Basic theory and application. *Comput. Methods Appl. Mech. Engrg.*, 139:289–314, 1996.
- [6] O. Laghrouche and P. Bettess. Short wave modelling using special finite elements. *J. Comput. Acoust.*, 8:189–210, 2000.
- [7] P. Ortiz and E. Sanchez. An improved partition of unity finite element model for diffraction problems. *Int. J. Numer. Meth. in Engrg.*, 50:2727–2740, 2000.
- [8] E. Giladi and J. B. Keller. A hybrid numerical asymptotic method for scattering problems. *Journal of computational Physics*, 174:226–247, 2001.
- [9] J. Trevelyan E. Perrey-Debain and P. Bettess. Plane wave interpolation in direct collocation boundary element method for radiation and wave scattering: numerical aspects and applications. *Journal of sound and vibration*, 261:839–858, 2003.
- [10] J. A. Monro Jr. O. P. Bruno, C. A. Geuzaine and F.Reitich. Prescribed error tolerances within fixed computational times for scattering problems of arbitrarily high frequency: the convex case. *Submitted to Royal Society*, 2003.
- [11] J.B.Keller. Rays, waves and asymptotics. *Bull. Am. Math. Soc.*, 84:727–750, 1978.
- [12] I.M. Babuška and J.M. Melenk. The partition of unity method. *Int. J. Numer. Meth. in Engrg.*, 40:727–758, 1997.
- [13] D.Givoli. *Numerical Methods for Problems in Infinite Domains*. Elsevier, 1992.
- [14] J. R. Mautz and R. F. Harrington. A combined-source solution for radiation and scattering from a perfectly conducting body. *IEEE Transactions on Antennas and Propagation*, 27(4):445–454, 1979.
- [15] J.B.Keller. Geometrical theory of diffraction. *J. Opt. Soc. Am.*, 52:116–130, 1962.
- [16] J.B.Keller. Diffraction by a convex cylinder. *Trans. IRE*, AP-4:312–321, 1956.
- [17] E. Giladi and J. B. Keller. An asymptotically derived boundary element method for the helmholtz equation. *In preparation*, 2003.